Ultrasonics Sonochemistry 92 (2023) 106248

Contents lists available at ScienceDirect

Ultrasonics Sonochemistry

journal homepage: www.elsevier.com/locate/ultson

Preparation and characterization of type 3 resistant starch by ultrasound-assisted autoclave gelatinization and its effect on steamed bread quality

Xiangyun Liu [a], Qianyun Ma [a,d,*], Dewei Cheng [a], Fan Zhang [a], Yuwen Li [a], Wenxiu Wang [a,d], Jie Wang [a,d], Jianfeng Sun [a,b,c,d,*]

[a] College of Food Science and Technology, Hebei Agricultural University, 289th Lingyusi Street, Lianchi District, Baoding 071000, China
[b] Hebei Potato Processing Technology Innovation Center, Hebei 076576, China
[c] Sino-US and Sino-Japan Joint Center of Food Science and Technology, Baoding, Hebei, China
[d] Hebei Technology Innovation Centre of Agricultural Products Processing, Baoding 071000, China

ARTICLE INFO

Keywords:
Resistant starch
Ultrasound
Autoclave gelatinization
Steamed bread

ABSTRACT

In this study, we aimed to establish an innovative and efficient preparation method of potato resistant starch (PRS). To achieve this, we prepared type 3 resistant starch (RS3) from native potato starch (PS) using an ultrasonic method combined with autoclave gelatinization and optimized by the response surface method to study the structure and properties of potato RS3 (PRS3) and its effect on the quality of steamed bread. Under optimal treatment conditions, the PRS3 content increased from 7.5% to 15.9%. Compared with PS, the B-type crystal structure of PRS3 was destroyed, and the content of hydroxyl groups was increased, but no new chemical groups were introduced. PRS3 had a rougher surface and a lower crystallinity, gelatinization temperature, viscosity, setback value, and breakdown value. The low content (5%) of PRS3 had a stable viscosity and was easily degraded by bacteria, which can improve the quality of steamed bread to a certain extent. When the PRS3 content was over 10%, it competed with the gluten protein to absorb water, which reduced the contents of β-turn and α-helix in the dough, increased the contents of β-fold, and weakened the structure of the gluten network. It also decreased the specific volume and elasticity of the steamed bread and increased the spreading rate, hardness, and chewiness. Steamed bread prepared with a flour mixture containing 5% PRS3 was similar to the presidential acceptance of control flour. In this study, a new sustainable and efficient PRS3 preparation method was established, which has certain guiding significance for the processing of Functional steamed bread with high-resistant starch.

1. Introduction

Resistant starch (RS) cannot be digested and absorbed until it reaches the colon [1], however, it can be degraded to short-chain fatty acids (SCFAs) in the colon by gut bacteria, adjusting the intestinal flora and metabolites to alleviate and prevent the occurrence of chronic diseases, including diabetes, colorectal cancer, kidney disease, and inflammation. Therefore, it can be inferred that diet plays a vital role in human health [2]. Moreover, resistant starch has a physiological function similar to dietary fiber and tastes the same as common starch, so it has great potential in the food and healthcare industries.

Resistant starch can be divided into five subtypes, which are RS1-5 as physically-embedded starch, raw resistant starch granules, retroactive starch, chemically modified starch, and starch-lipid complex respectively [3]. Preparing RS4 and RS5 requires the addition of many chemically modified reagents or structural modifiers, which are potentially unsafe for human beings. RS3 is prepared by heating and physically pasting starch without using chemical reagents; it has good thermal stability, controllable production, and strong resistance to enzymatic hydrolysis [4]. However, preparing RS3 by single gelatinization or enzymatic degradation has many disadvantages, such as a long processing time and a low conversion rate [3]. Therefore, there is a need for

* Corresponding authors at: College of Food Science and Technology, Hebei Agricultural University, 289th Lingyusi Street, Lianchi District, Baoding 071000, China.
E-mail addresses: maqianyun@126.com (Q. Ma), causunjf@hebau.edu.cn (J. Sun).

https://doi.org/10.1016/j.ultsonch.2022.106248
Received 19 October 2022; Received in revised form 14 November 2022; Accepted 27 November 2022
Available online 28 November 2022

a simple and environmentally friendly method for the industrial production of RS, especially RS3. Currently, most studies use ultrasonic microwave radiation and combined enzymatic hydrolysis to prepare resistant starch [5,6]; there are few studies on the preparation of resistant starch by combining ultrasonic radiation with pressure and heat.

Potato is the fourth largest crop in the world. According to data from the China Bureau of Statistics in 2021, the country's potato production reached 1,830.9 million tons, mainly used in fresh and processed foods such as potato chips and chips. Meanwhile the dry base content of potato starch is about 75 % [7], which is a good source of resistant starch. Alternatively steamed bread is an indispensable staple in the daily diet of northern China. Therefore, it is important to develop functional steamed bread with a high level of resistant starch. Gao et al. studied the effects of the starch-monoglyceride complex (WSG) on the specific volume, elasticity, spread rate, hardness, and chewability of steamed bread [8]. Haini et al. studied the influence of RS2 on the rheological and physicochemical properties, nutritional value, digestive characteristics of steamed bread [9]. However, there are few reports regarding RS3 in steamed bread.

To solve the above problems, this study aimed to establish an innovative and efficient preparation method of potato resistant starch (PRS). We used response surface methodology (RSM) to optimize the processing parameter. We studied the effects of ultrasound and autoclave gelatinization on the molecular structure, crystallinity, and gelatinization of PRS. We also assessed the effect of PRS content on the appearance, quality, texture, and sensory evaluation of steamed bread. Our findings can expand the potential application of potato starch and provide a theoretical basis and technical support for the industrial production and application of RS3.

2. Materials and methods

2.1. Materials and chemicals

All reagents were of analytical grade except for the following: potato starch (26 % amylose,72 % amylopectin, 15.8 % moisture content) containing 7.5 % RS (Sichuan Youjia Foodstuffs Co., ltd., China); wheat flour (Jin Sha He Co., ltd., China); instant dry yeast (Angel Yeast Co., ltd.); *Aspergillus oryzae* (100 U/mg, Beijing Biotopped Sci-Technology Co., ltd., China); and glucoamylase (100,000 U/mg, Beijing Solarbio Co., ltd., China).

2.2. Process optimization of PRS

2.2.1. Preparation method of resistant starch

Potato starch (PS) was mixed with distilled water to form a slurry; the pH of the slurry was adjusted, and then, the slurry was treated with an ultrasonic instrument (SB-5200 DTD; Scientz, Ningbo, China) at 50 ℃. Subsequently, the slurry was subjected to autoclave gelatinization in an autoclave (DSX-30L-I, SHENAN, Shanghai, China) at 121 °C. The slurry was then cooled in cold water to about 25 ℃. After retrogradation at 4 °C, it was freeze-dried in a vacuum, crushed, and screened through 50 mesh to produce the finished product.

2.2.2. Resistant starch content

The method was slightly modified according to the method of Yang et al [10]. The sample (1.000 ± 0.001 g) was weighed, and 10 mL citric acid-sodium citrate buffer (pH = 5.8) and 0.1 g high-temperature α-amylase were added. The mixture was heated in a water bath at 90 °C for 30 min. Subsequently, the mixture was subjected to 100 °C for 15 min to deactivate the enzyme, then cooled and centrifuged (3000 rpm, 20 min), the supernatant was discarded, and 10 mL acetic acid-sodium acetate buffer (pH = 4.5) and 0.1 g glucose amylase were added to the precipitate, which was heated in a water bath at 60 °C for 30 min. Subsequently, the sample was subjected to 100 °C for 15 min to deactivate the enzyme and then cooled and centrifuged (3000 rpm, 20 min). The supernatant was discarded, and the precipitate was washed with water. This process was repeated three times. Then, 10 mL of 2 mol/L KOH was pipetted into the precipitate, which was allowed to rest for 30 min. Then, 5 mL citric acid-sodium citrate buffer and 0.1 g high-temperature α-amylase were added, and the mixture was bathed in water at 90 °C for 30 min. Subsequently, the mixture was kept at 100 °C for 15 min to deactivate the enzyme before it was cooled to about 25 ℃ and the pH was adjusted to 4.5. Glucose amylase (0.1 g) was added to the mixture, which was then heated in a water bath at 60 °C for 30 min and then kept at 100 °C for 15 min to deactivate the enzyme. The mixture was then cooled and centrifuged (3000 rpm, 20 min), the precipitate was washed three times with distilled water and the supernatant was used for determination. The supernatant was added to distilled water to make a volume of 100 mL. The content of reducing sugar in the solution was determined by the 3́, 5-dinitrosalicylic acid (DNS) method; the yield of resistant starch was multiplied by 0.9. The experiments were repeated three times.

2.2.3. Single factor experiment

Total resistant starch content (TRS) of the potato was investigated under various Starch slurry content (10 %, 15 %, 25 %, 30 %, 35 %, 40 %), pH of the slurry (4, 5, 6, 7, 8), ultrasonic power (180, 210, 240, 270, 300 W), ultrasonic time (0, 15, 30, 60, 80, 90 min), autoclave gelatinization time (10, 20, 30, 45, 90, 120 min), and retrogradation time (4, 12, 18, 24, 36 h). Each test was repeated three times.

2.2.4. RSm

Based on a single-factor test, for which the design and specific parameters are listed in Table S1, the Box–Behnken method was used for the three-factor and three-level experimental design. The autoclave gelatinization time (A), ultrasonic time (B), and starch slurry content (C) were considered the experimental parameters, and total resistant starch content (TRSC) was regarded as the response value. The factor levels and codes are presented in Table 2.

2.3. Determination of physicochemical properties of optimized PRS3

2.3.1. Gelatinization characteristics

The gelatinization characteristics of samples were determined according the method of Antonella Pasqualone et al. [11] with slight modifications using Viscograph-E (Brabender, Germany). Sample (30 g) was suspended in 450 mL distilled water. After moisture correction, heating and cooling cycles were performed, starting at 30 °C, reaching a temperature of 95 °C and maintaining that temperature for 8 min, and finally cooling to 50 °C and maintaining that temperature for 5 min, heating/cooling rate was 1.5 °C/min.

2.3.2. Fourier-transform infrared spectroscopy (FTIR)

The freeze-dried powder sample (2 mg) was placed in a mortar containing KBr (200 mg) and dried at 105 °C for 24 h. After fully grinding, the powder was pressed into 1 – 2 mm slices. The full-scanning mode of FTIR (IRAffinity-1S, Shimadzu Enterprise Management Co., ltd., Shanghai, China) was used, the scanning wavelength was set as 400 – 4000 cm^{-1}, and the scanning resolution at 4 cm^{-1}. The resulting original infrared spectrum was calibrated and deconvolved using Omnic software (Thermo Fisher Scientific, Waltham, MA, USA). The deconvolved half-peak width was 20 cm^{-1}, the enhancement factor was 2.4, and the intensity ratio was calculated at 1047 to 1015 cm^{-1} [12].

2.3.3. Scanning electron microscopy (SEM)

The starch powder was fixed to the aluminum plate with double sticky tape and was then sprayed gold under vacuum. The morphological characteristics of the starch samples were evaluated by SEM (Tescan VEGA3 SBH, Shanghai, China) at 1200× and 2200× magnifications at 1.0 kV acceleration voltage.

2.3.4. X-ray diffraction (XRD)

Starch samples were measured by XRD (D2 PHASER, Bruker AXS, Germany) according to the method of Wang et al. [10] with minor modifications. The diffractometer was set at 40 kV and 40 mA. The diffractograms were collected over a 2θ range from 5° to 40° with a step length of 0.02° and a scanning rate of 4°/min. Crystallinity was calculated using Origin 2019 software.

2.4. Preparation and property determination of steamed bread of PRS

2.4.1. Preparation of the steamed bread

PRS3 was mixed with wheat flour in proportions of 0, 5, 10, 15, and 20 % (w/w) to make steamed bread. Yeast powder (5 g) was dissolved in a small amount of warm water, and the total volume was made up to 150 mL. The liquid was then added to 300 g of the mixture and stirred into a flocculent mixture with chopsticks. The dough was kneaded by hand for 15 min until smooth and formed and then placed into a proofing box at 38 °C with 85 % humidity to proof for 60 min. After proofing, the dough was divided into six 50 g pellets and rounded into balls, which were left to proof for 5 min before being placed into a boiling pot and steamed for 30 min. After removing from the pot, the steamed bread was cooled to 25 ℃, and was assessed immediately.

2.4.2. Determination of specific volume and color

The cooled steamed bread was weighed, and its diameter and height were measured. The volume of the bread was determined by the millet displacement method. The specific volume was equal to the ratio of volume (mL) to weight (g), and the spread ratio was equal to the ratio of diameter (cm) to height (cm).

2.4.3. Texture profile analysis (TPA)

Using the method described by Sim et al. [13] with minor modifications, steamed bread was evaluated using the TA.XTplus Texture Analyzer (FTC Co., ltd., Sterling, VG, US). The steamed bread was cut into thick slices (~20 mm) for texture determination. A cylindrical probe with a diameter of 35 mm compressed the sliced steamed bread to 75 % deformation. The speed was 1 mm/s in test. The interval time was 10 s between two tests, and the triggering force was 5 g. The results of the three tests were averaged for all samples.

2.4.4. Determination of secondary structure contents

After vacuum freeze-drying, the dough was crushed. Fourier determination was performed on the dough samples according to the method described in 2.2.7. The amide I band (1600–1700 cm^{-1}) was analyzed and cut by PeakFit software (Palo Alto, CA, USA), and baseline correction, Gaussian deconvolution, and second derivative fitting were performed to minimize the residual error. Finally, the proportion of each secondary structure of the gluten protein was determined by peak area [14,15].

The corresponding relationship between the wave number of amide I with the characteristic peaks and secondary structure of gluten protein were as follows: α-helix, 1646–1664 cm^{-1}; β-folding, 1615–1637 cm^{-1} and 1685–1700 cm^{-1}; β-angle, 1665–1684 cm^{-1}; random crimp, 1637–1645 cm^{-1} [16].

2.4.5. Sensory evaluation

Ten experts conducted a sensory evaluation on the steamed bread, scoring it out of 100 points; the final score was averaged. Sensory scoring criteria were slightly modified from the GB/T 35991-2018 (Chinese National Standard) method, as shown in Table 1.

2.5. Statistical analysis

SPSS 13.0 was used for significance analysis, Origin 2019 was used to draw images, and Design-Expert 8.0.6.1 software was used for the RSM design and result analysis. Secondary structure data were processed with the software Peakfit V4, and all experiments were repeated at least three times. Data are expressed as means and standard deviations.

Table 1
Sensory scoring criteria of steamed bread.

Parameters	Scores	Evaluation rules
Color	10	Uniform milky white(8–10);Medium (4–7); Uneven and severe yellowing 1–3
Surface morphology	15	Smooth skin, symmetrical shape (11–15);Medium (6–10); Rough skin, bubble and cracks in surface 1–5
Structure Internal texture	15	Small and homogenous genous,Good layers (11–15); Medium (6–10);Stomata large and uneven or too compact, cellular structure (1–5).
Elasticty	15	Bite strength, good recovery after extrusion (11–15); Medium (6–10);Bounce back difficultly when pressed with finger (1–5).
Hardness	15	Soft and moderate 11–15;Medium (6–10); Not soft, chewing hard 1–5
Stickiness	10	Refreshing and not sticky, delicate taste (8–10);A little sticky or sticky (3–7);not refreshing and sticky (1–3)
Taste	10	Delicious, chewing sweet (8–10);Medium (4–7);a bitter taste (1–3).
Flavor	10	Pleasant steamed bread scent (8–10);Medium (4–7);Unpleasant smell (1–3).

3. Results and discussion

3.1. Response surface optimization experiment results

On the basis of single factor (Figure S1), response surface methodology (RSM) was used to optimize the production process and the optimal PRS production process was obtained. The specific scheme and results of the central combined test are shown in Table 2. There are 17 experimental sites, including 12 factorial tests and 5 central tests. The central repeated tests are used to estimate test errors. Multivariate fitting regression analysis was performed for each group of data in Table 2, and the fitting equation was obtained as follows:

Y = 16.07–1.51B-0.76AC-1.6A2-1.99B2-3.73C2.

The results of variance analysis are shown in Table3. The model P

Table 2
Factors and levels used in Box-Behnken experimental design.

Run	A(min)	B(min)	C (%)	TRSC (%)
1	0(92.5)	0(80)	0(30)	15.43
2	0(92.5)	0(80)	0(30)	15.70
3	−1(75)	0(80)	1(35)	11.09
4	0(92.5)	0(80)	0(30)	16.57
5	1(110)	0(80)	−1(25)	11.93
6	0(92.5)	1(85)	−1(25)	8.92
7	1(110)	1(85)	0(30)	11.81
8	−1(75)	0(80)	−1(25)	10.07
9	1(110)	0(80)	1(35)	9.90
10	−1(75)	1(85)	0(30)	10.73
11	0(92.5)	0(80)	0(30)	16.86
12	0(92.5)	−1(75)	1(35)	11.81
13	0(92.5)	−1(75)	−1(25)	12.51
14	1(110)	−1(75)	0(30)	14.20
15	0(92.5)	0(80)	0(30)	15.80
16	−1(75)	−1(75)	0(30)	13.21
17	0(92.5)	1(85)	1(35)	8.20

Table 3
Results of variance analysis on the influence of RS preparation parameters.

Source	Sum of Squares	df	Mean square	F Value	P-value Prob > F	significant
Model	116.32	9	12.92	37.11	<0.0001	**
A	0.94	1	0.94	2.69	0.1447	
B	18.21	1	18.21	52.28	0.0002	**
C	0.74	1	0.74	2.12	0.1888	
AB	2.025E-003	1	2.025E-003	5.810E-03	0.9414	
AC	2.33	1	2.33	6.68	0.0363	**
BC	1.000E-004	1	1.000E-004	2.871E-04	0.9870	
A^2	10.76	1	10.76	30.89	0.0009	**
B^2	16.61	1	16.61	47.68	0.0002	**
C^2	58.46	1	58.46	167.83	< 0.0001	**
Residual	2.44	7	0.35			
Lack of Fit	0.94	3	0.31	0.84	0.5372	not significant
Pure Error	1.49	4	0.37			
Cor Total	118.76	16				
Coefficient of determination (R^2_{adj}) = 0.9531						

Note: *, the difference is significant (P < 0.05), **, the difference is extremely significant (P < 0.01).

value reached extremely significant level (P < 0.0001), indicating that the regression equation reaches an extremely significant level. The mismatch term was not significant (P = 0.5372 > 0.05). The calibration coefficient R^2_{adj} was 0.9531 and indicating that the model can explain 95.31 % of the response value changes. Therefore, this model can be used to analyze and predict PRS production. According to the F value of each factor, the influence sequence of each factor on the response value was B > A > C.

Fig. 1 described the three-dimensional diagram and contour diagram of the response surface, which intuitively reflects the influence of various factors on TRSCD. Fig. 1A-F shows that the contour lines of starch slurry content and ultrasonic time, as well as starch slurry content and autoclaved gelatinization time tend to be elliptical. This shows that the interaction between them is obvious. The contour lines of ultrasonic time and autoclaved time tended to be round, indicating that the interaction between the two is not obvious. This is consistent with the results in Table 3.

Based on the Box-Behnken design, the ideal test conditions were obtained as follows: 95 min of autoclave gelatinization time, 78 min of the ultrasonic time, and 30 % of Starch slurry content. Under these conditions, the content of resistant starch was 16.386 %. Under these conditions, corresponding experimental PRS3 was 15.92 %, which indicated that the model fitted well with the actual situation and the results were reliable and valuable for reference.

3.2. Physicochemical characteristics of the optimized PRS

3.2.1. SEM results

The morphological characteristics of starch were observed by SEM. As demonstrated in Fig. 2, the PS particles had a round or oval-shaped structure with a mostly smooth surface. However, the PRS particles maintained an irregular block structure with a folded surface, and the particle size was significantly larger than PS, indicating that the original particle structure of the PS had been destroyed after the reinforced physical field process, and a more stable crystal structure had been formed during the retrogradation stage.

The occurrence of α-1, 6 glycosidic bond breakage and the cavitation phenomenon caused by ultrasonic treatment resulted in very high pressure and shear force. Consequently, this caused mechanical degradation of the amorphous and crystalline layer outside the starch particles [17]. After pressure heat gelatinization, starch granule overexpansion leads to the cleavage of its complete structure and the leakage of the amylose chain. During regeneration, the disordered and

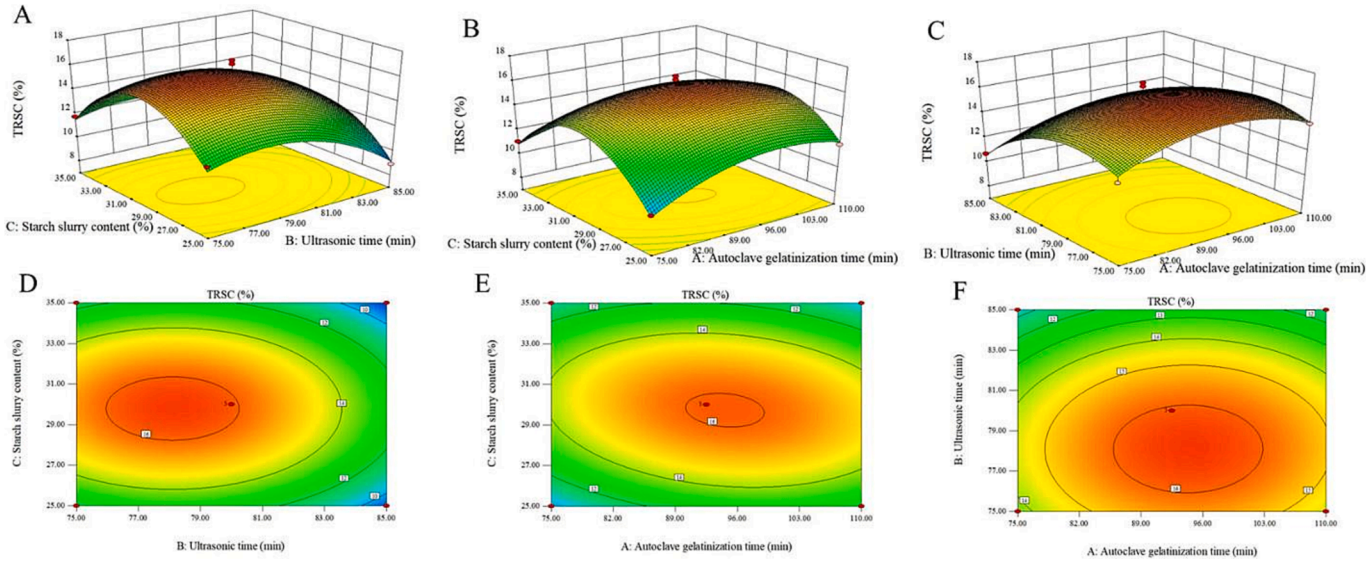

Fig. 1. A–C: The response surface 3d map of the interaction between Starch slurry content and Ultrasonic time (A), Starch slurry content and Autoclave gelatinization time (B), Ultrasonic time and Autoclave gelatinization time (C); D-F: The response surface contour map of the interaction between Starch slurry content and Ultrasonic time (D), Starch slurry content and Autoclave gelatinization time (E), Ultrasonic time and Autoclave gelatinization time (F).

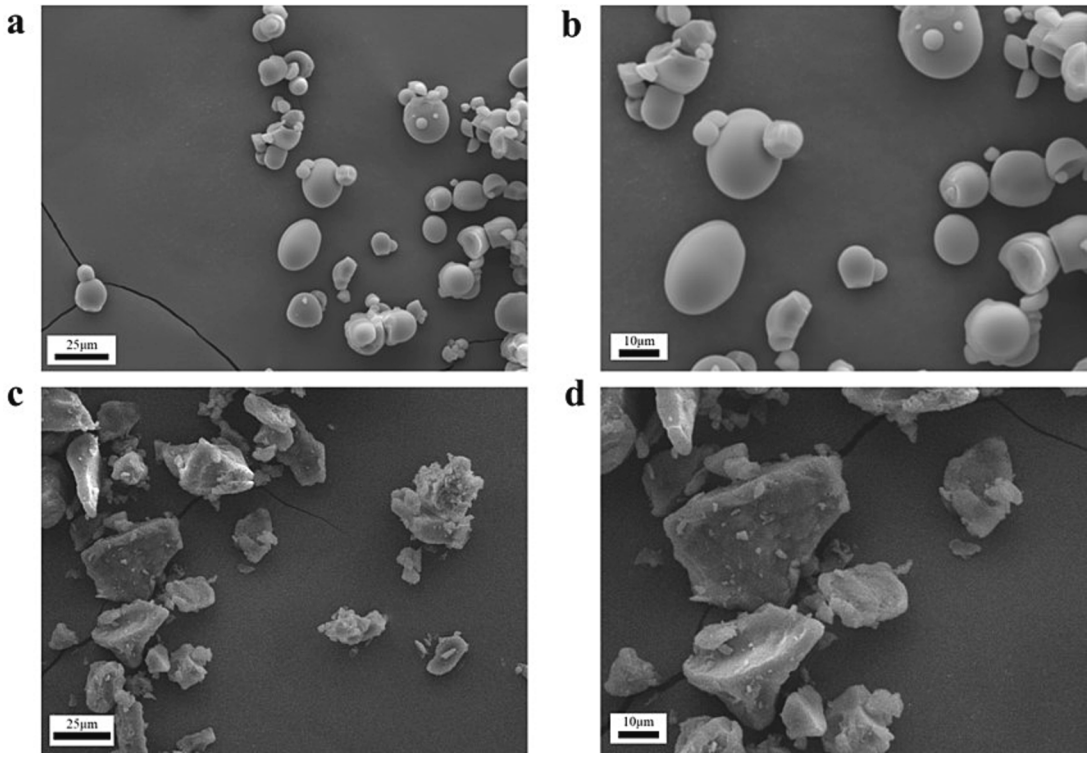

Fig. 2. Scanning electron microscope images of PRS and PS. (a) PS (×1200); (b) PS (×2200); (c) PRS (×1200); (d) PRS (×2200).

freely coiled amylose chains re-form the double helix structure through hydrogen bonding and hydrophobic forces. The tiny crystal nuclei formed by the superposition of the double helix grow and mature continuously, and eventually form large, coarse, and irregular recombination particles [18]. The recrystallization structure reduces the binding target of starch digestive enzyme activity groups and starch molecules [19], thereby strengthening the anti-enzyme resolution of PRS.

3.2.2. FTIR spectroscopy analysis

The structural changes of starch samples can be monitored by FTIR spectroscopy, providing information for short-range sequencing [20]. FTIR spectra of starch samples were shown in Fig. 3A. The spectral lines of PRS and PS have the same trend, with characteristic peaks appearing at 1024.44 cm^{-1}, 1157.42 cm^{-1}, 1647.08 cm^{-1}, 2928.86 cm^{-1}, and approximately 3200 cm^{-1}. The absorption peak between 800 and 1200/cm^{-1} was caused by the stretching vibration of C—C, C-OH, and C—H; the absorption peak at 1647.08 cm^{-1} reflected the C═O vibration; the absorption peak at 2928.86 cm^{-1} reflected the C—H stretching vibration; the absorption peak at 3200 cm^{-1} reflected the O—H stretching vibration. The peak near 2358 cm^{-1} was due to the C═O stretching vibration of carbon dioxide in the air [21]. The shape and position of the spectral peaks of all starch samples were similar. No new functional groups were formed during the production of PRS, and only the ordered rearrangement of the PS molecular chain was observed. However, compared with PS, the intensities of the bands increased for PRS at 3200 cm^{-1}. This may be due to the hydrogen bonding effect of ultrasonic treatment on starch molecules, which increases the hydroxyl content and the hygroscopicity of PRS, and is consistent with the results of gelatinization properties.

The absorbance ratio of 1047 cm^{-1} and 1022 cm^{-1} of FTIR spectra can be used to reflect the short-range ordered structure. The absorbance

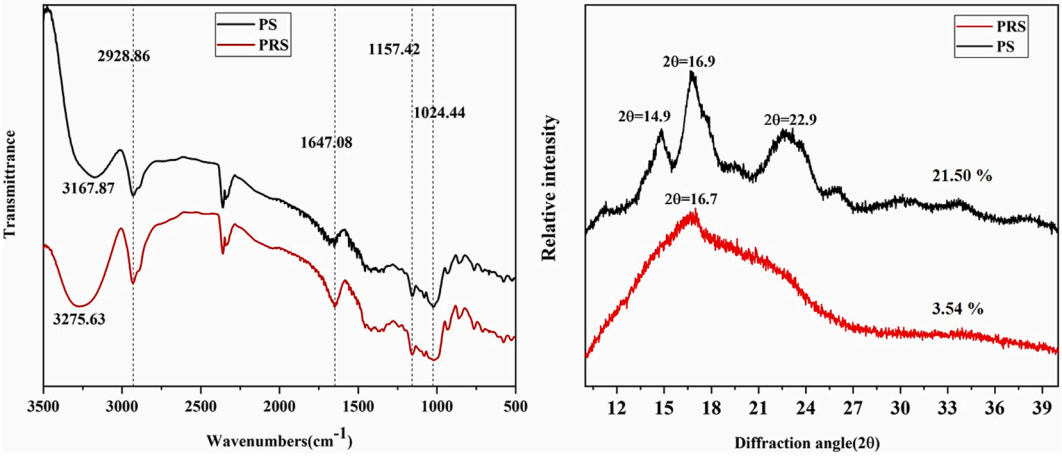

Fig. 3. (a) Infrared spectrum scanning of potato starch and resistant potato starch; (b) X-ray diffraction patterns of resistant starch.

ratio of PRS (0.78 ± 0.15) was significantly lower than that of PS (1.25 ± 0.11), which may be caused by the destruction of hydrogen bond association in the crystallization region of starch under the conditions of ultrasound and autoclave gelatinization, exposing more of the double-helix structure, thereby reducing the proportion of the crystallization region [22].

3.2.3. XRD analysis

The differences in crystal deconstruction and crystallinity between PRS and PS were studied by XRD, which can reflect the change in the long-range ordered structure of the starch molecule. As shown in Fig. 3B, PS has strong diffraction peaks at 14.9°, 16.9°, and 22.9°, indicating that PS is a B-type tuber starch, consistent with the reports of Li et al. [23] and Li et al. [24]. However, compared with PS, the XRD pattern of PRS was greatly changed with only a strong peak at 16.9°; the rest of the peak had almost disappeared, showing the characteristics of an amorphous dispersion diffraction peak. This indicates that the crystalline structure of PS after ultrasonic and autoclave gelatinization treatment had been destroyed, and the starch particles had changed from a polycrystalline structure to an amorphous structure. The software JADE was used to calculate the starch crystallinity. The crystallinity of PS was significantly higher than that of PRS, which is consistent with the above FTIR results and the findings of Seid et al. [20,25], indicating that the degree of crystallinity had little influence on the enzymatic hydrolysis resistance of starch.

3.2.4. Gelatinization characteristics

The change in starch gelatinization viscosity is related to the hydration, breakage, and chain association of starch particles at high temperatures. The gelatinization temperature, peak viscosity, final viscosity, decomposition value, and setback value of potato resistant starch were lower than those of the original potato starch group (Table 4). The decrease in gelatinization viscosity caused by ultrasound and pressure heat treatment may be due to the reduced starch expansion force, resulting in a reduced volume fraction caused by the degree of association between starch chains and the reduced diffusion of amylopectin molecules [26]. The gelatinization temperature of PRS was significantly lower than that of the PS group, indicating that PRS had a strong water absorption ability. The final viscosity reduction indicates that PRS had a better chewing sensation. The decrease in breakdown value indicated that the composite had stronger shear resistance and higher thermal stability [27]. The reduction in the regeneration value indicates that RS has a better anti-regeneration ability [28], which can improve food quality, taste, and shelf life.

3.3. Effects of resistant starch on the properties of steamed bread

3.3.1. Quality of steamed bread.

Specific volume and spread ratio are objective indexes used to evaluate the quality of steamed bread. The effect of resistant starch on steamed bread quality was shown in Table 5. The content of PRS had a significant influence on the spread ratio and specific volume. With the increase of PRS addition, the spread ratio showed an increasing trend. However, the specific volume of steamed bread decreased from 1.77 to 1.32, except in the 5 % group. When the amount of PRS was 5 %, the specific volume was significantly higher than the control group. However, when the content of resistant starch was<10 %, the color of steamed buns could be significantly improved. As shown in Fig. 4, there was no significant difference in the shape of the steamed buns. However, when the amount of resistant starch added was more than 5 %, the steamed buns gradually showed large and uneven pore distribution and a surface that became more cracked with the increase in the resistant starch content. This was mainly because of the quality of steamed bread depends mainly on the quantity and quality of gluten proteins [29]. PRS, with stable adhesion, can gather the molecules in the dough during steaming, enhancing air retention, and thereby increasing the volume of steamed bread. RS is a prebiotic, which can increase yeast activity and the volume of steamed bread. However, when the content of PRS was too high, it competed with gluten for water absorption resulting in the excessive dilution of gluten protein. Gas retention reduction thereby reducing the specific volume [30].

Table 5
Effects of the addition amount of PRS on quality of steamed bread.

Sample	volume(mL)	Specific volume	Spread ratio	L*
0 %	88.62 ± 0.36^{b}	1.77 ± 0.01^{b}	1.13 ± 0.01^{c}	83.56 ± 1.16^{ab}
5 %	91.46 ± 2.31^{a}	1.83 ± 0.05^{a}	1.14 ± 0.02^{bc}	83.6 ± 1.33^{ab}
10 %	79.63 ± 1.41^{c}	1.59 ± 0.03^{c}	1.14 ± 0.01^{bc}	84.07 ± 0.25^{a}
15 %	72.85 ± 0.32^{d}	1.46 ± 0.01^{d}	1.15 ± 0.01^{ab}	83.52 ± 0.33^{ab}
20 %	65.87 ± 1.44^{e}	1.32 ± 0.03^{e}	1.16 ± 0.01^{a}	82.2 ± 0.28^{b}

Note: Values are means ± standard deviation (n = 3). Different letters represent significant differences between different treatment groups at the same storage time.

3.3.2. Texture profile analysis (TPA)

The influence of resistant starch on the texture characteristics of steamed bread was presented in Fig. 5. With the increase in PRS content, the hardness showed a significant increasing trend from 251 N to 358.93 N. However, lower proportions of PRS had a positive effect on the hardness of the steamed bread when 5 % PRS was added, the hardness decreased from 251.43 N to 239.55 N. The data show that hardness and chewiness had a similar positive correlation, probably because PRS cross-links with gluten protein through covalent bonds and hydrogen bonds to reduce the destruction of disulfide bonds, thereby strengthening the gluten network structure and reducing the hardness of the steamed bread [31]. However, as the proportion of PRS increases from 10 % to 20 %, the gluten cohesiveness was strengthened by combining proteins [30,32], increasing the polymerization of gluten proteins and the formation of polymers. This is the major reason for the increasing hardness of steamed bread. The change in hardness was consistent with the volume of steamed bread.

The adhesiveness of the steamed bread reflected the mouthfeel of steamed bread. The adhesiveness of the <5 % PRS group is not significantly different from that of the control group. This indicates that when the amount of PRS was below 5 %, the mouthfeel of steamed bread cannot be affected due to the water absorption of resistant starch and the gelatinization of starch at the steaming stage [33]. The resilience, elasticity and cohesiveness decreased with greater PRS content. This may be due to gluten dilution caused by steric hindrance of PRS [34] and

Table 4
Gelatinization characteristics of RS and PRS.

Sample	Gelatinization Temperature (℃)	Initial viscosity (BU)	Peak viscosity (BU)	Final viscosity (BU)	Breakdown (BU)	Setback (BU)
PS	65.17 ± 0.76	12.23 ± 0.13	880.33 ± 7.51	783.67 ± 8.62	337.67 ± 1.53	243.33 ± 1.53
PRS	53.40 ± 0.10	11.41 ± 0.24	73.33 ± 0.58	105.67 ± 1.53	14.33 ± 1.53	45.67 ± 1.53

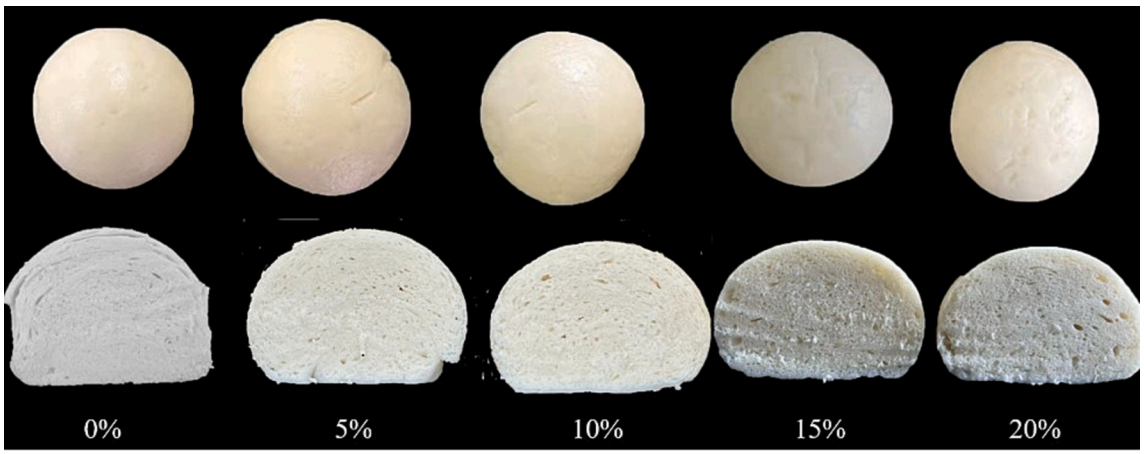

Fig. 4. Pictures of streamed bread appearances and textures.

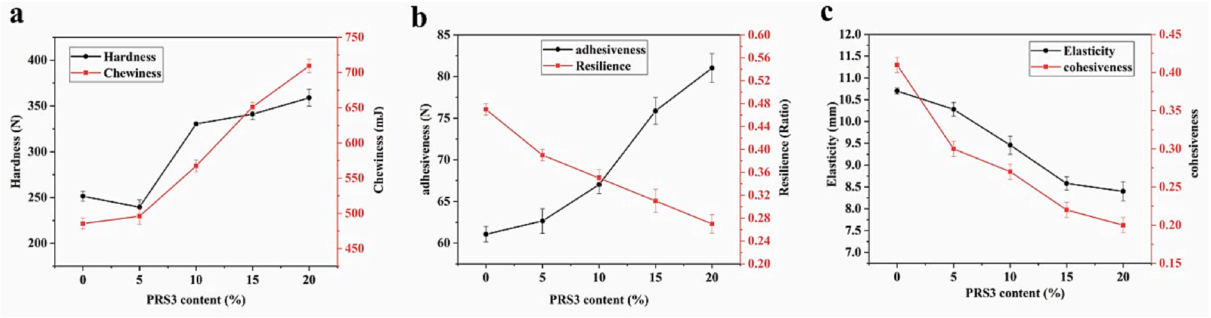

Fig. 5. Effects of the addition amount of PRS on texture of steamed bread.

the high amylose content of RS. The amylose chains cannot leach out of the granules to form an interconnected network [35].

3.3.3. *Gluten protein structure of the dough*

Gluten content is one of the most important factors affecting the quality of dough; the configuration of protein molecules is affected by changes in the secondary structure of the protein [36]. As shown in Fig. 6, β-sheets had the highest percentage of protein secondary structure, followed by β-turns and α-helixes in the dough without PRS.

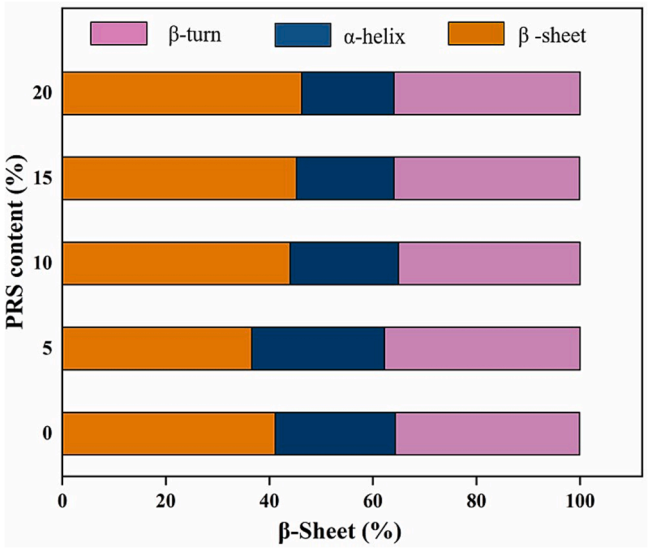

Fig. 6. Effects of the addition amount of PRS on secondary structure contents.

When the PRS content was 5 %, the percentage of β-sheets and α-helixes in the secondary structure of the dough protein was significantly increased. When the content of PRS was higher than 5 %, the percentage of β-sheet in the secondary structure of the dough protein increased, while the percentage of α-helix decreased; the percentage of β-turn did not change significantly. These results indicated that PRS had a significant effect on the β-sheet and α-helix regions in the protein secondary structure of the dough. Low PRS content can improve the quality of steamed bread by altering the protein secondary structure. Gluten is formed gradually through hydration during mixing and standing. With an increase in gluten hydration, the gluten network formed completely, and the percentage of β-sheets decreased, while the percentage of β-turns and α-helixes increased [37]. In particular, an increase in the α-helix content increases the stability of the gluten protein. However, a higher content of PRS has a stronger water absorption, which leads to competition with the gluten protein to absorb water, weakening the water compatibility of the gluten protein, and resulting in an increase of the percentage of β-sheets and a decrease in the percentage of α-helixes. Ultimately, this weakens the structure of the gluten network and leads to a decline in the quality of steamed bread (Fig. 7).

3.3.4. *Sensory evaluation of steamed bread*

Sensory evaluation of food is used to describe and judge food quality, reflecting the requirements of food enjoyment and edibility. The overall acceptability of the steamed bread was obtained by dividing the total score by the number of indicators. The sensory scores of the steamed bread were shown in Fig. 1. When the amount of PRS was <5 %, there was no significant difference in the sensory score of the steamed bread. However, when the amount of PRS added was more than 10 %, the sensory score of the steamed bread was negatively correlated with the amount of PRS added. When the PRS content was 20 %, the sensory score dropped to 48.8 (<60), severely affecting people's acceptance of

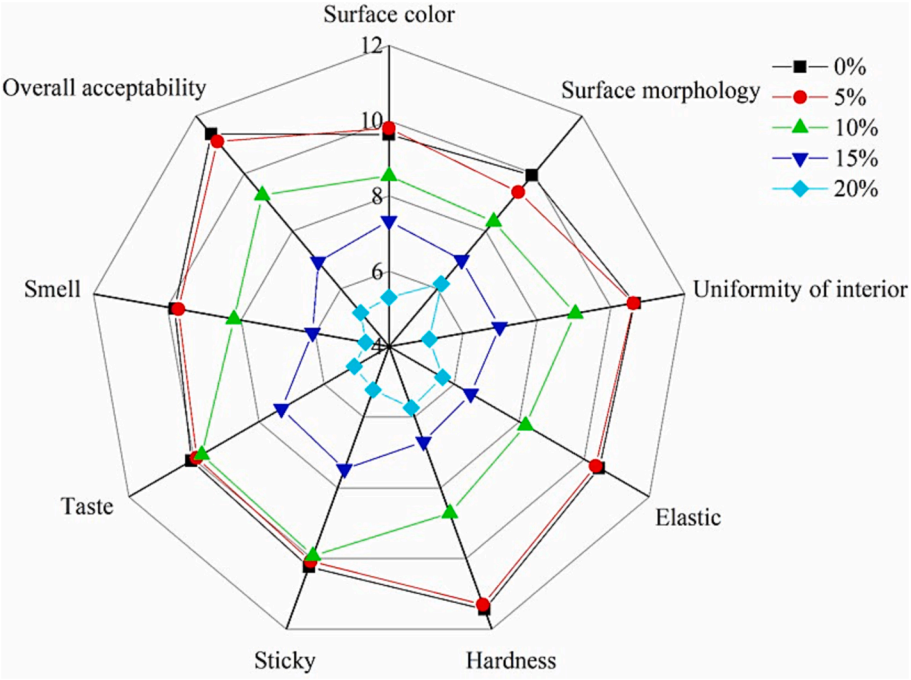

Fig. 7. The radar map of steamed bread sensory evaluation.

steamed bread. The main reason for this drop is that the addition of RS caused a deterioration in the internal structure of the steamed bread and caused excessive fermentation; this resulted in a sour taste and yellow color, which affected the mouthfeel and appearance.

4. Conclusions

Our study revealed that ultrasound-assisted autoclave gelatinization is a simple, environmentally friendly method to efficiently produce PRS. Compared with the original starch, TRSC was doubled under optimal conditions. Moreover, PRS3 has good thermal stability, strong water absorption, expansion ability, shear resistance. Meanwhile, the B-type crystal structure of PRS3 processed by the strong, physical field of ultrasonic treatment and pressure heat treatment is destroyed, with reduced crystallinity and short-range order. However, no new chemical groups are introduced, and its apparent shape changes from the original smooth sphere to a rough lump. Excessive substitution of PRS had negative effects on the specific volume, elongation, color, hardness, chewiness, elasticity, and other qualities of the steamed bread. However, low content of PRS3 can shorten the fermentation time of steamed bread and improve the network structure and color. Consequently, ~5% PRS3 is suggested to make functional steamed bread. Nonetheless, future work could focus on the effect of RS level on the steamed bread fermentation process.

CRediT authorship contribution statement

Xiangyun Liu: Conceptualization, Methodology, Data curation, Investigation, Writing – original draft, Writing – review & editing, Supervision. **Qianyun Ma:** Conceptualization, Methodology, Writing – review & editing, Supervision. **Dewei Cheng:** Data curation, Methodology, Supervision. **Fan Zhang:** Investigation, Supervision. **Yuwen Li:** Investigation, Supervision. **Wenxiu Wang:** Investigation, Resources, Supervision. **Jie Wang:** Investigation, Resources, Supervision. **Jianfeng Sun:** Conceptualization, Methodology, Data curation, Investigation, Supervision.

Declaration of Competing Interest

The authors declare that they have no known competing financial interests or personal relationships that could have appeared to influence the work reported in this paper.

Acknowledgements

This work was financially supported by the Program of the Hebei Youth Top-notch Talent Supporting Plan (0316027), the Young Scholar Scientific Research Foundation of Hebei Agricultural University (YJ201946), Hebei Province “Three Three Three” Talent Project (A202005002), the Research of Key Technologies and Development of Product for Comprehensive Utilization of Potato (20327103D) and Hebei Province Modern Agricultural Industry Technology System Open Field Vegetable Innovation Team Project (HBCT2021200207).

Appendix A. Supplementary data

Supplementary data to this article can be found online at https://doi.org/10.1016/j.ultsonch.2022.106248.

References

[1] N. Noor, A. Gani, F. Jhan, J.L.H. Jenno, M. Arif Dar, Resistant starch type 2 from lotus stem: ultrasonic effect on physical and nutraceutical properties, Ultrason. Sonochem. 76 (2021) 105655.
[2] G. Hu, Qiao, Q. Tuomilehto, J. Balkau, B. Borch-johnsen, Prevalence of the metabolic syndrome and its relation to all-cause and cardiovascular mortality in nondiabetic European men and women, Arch. Intern. Med. 164 (2004) 1006–1076, https://doi.org/10.1001/archinte.164.10.1066.
[3] L.B. Bindels, J. Walter, A.E. Ramer-Tait, Resistant starches for the management of metabolic diseases. Curr. Opin. Clin. Nutr. Metab. Care 18 (6) (2015) 559–565.
[4] Jiang, Wang, Luo, et al., Design and application of highly efficient flame retardants for polycarbonate combining the advantages of cyclotriphosphazene and silicone oil, Polymers 11 (7) (2019) 1155.
[5] K. Zhang, D. Zhao, D. Guo, X. Tong, Y. Zhang, L. Wang, Physicochemical and digestive properties of A- and B-type granules isolated from wheat starch as affected by microwave-ultrasound and toughening treatment, Int. J. Biol. Macromol. 183 (2021) 481–489.
[6] Z.-H. Lu, N. Belanger, E. Donner, Q. Liu, Debranching of pea starch using pullulanase and ultrasonication synergistically to enhance slowly digestible and resistant starch, Food Chem. 268 (2018) 533–541.

[7] V. Bártová, J. Bárta, A. Brabcová, Z. Zdráhal, V. Horáčková, Amino acid composition and nutritional value of four cultivated South American potato species, J. Food Compos. Anal. 40 (2015) 78–85.
[8] M. Shi, F. Wang, P. Lan, Y. Zhang, M. Zhang, Y. Yan, Y. Liu, Effect of ultrasonic intensity on structure and properties of wheat starch-monoglyceride complex and its influence on quality of norther-style Chinese steamed bread, LWT- Food Science 138 (2021) 110677.
[9] N. Haini, L. Jau-Shya, R. George Mohd Rosli, H. Mamat, Effect of type-2 resistant starch (high-amylose maize starch) on the physicochemical, nutritional, in vitro starch digestibility and estimated glycaemic properties of Chinese steamed buns, J. Cereal Sci. 98 (2021) 103176.
[10] Y. Yang, Q. Chen, A. Yu, S. Tong, Z. Gu, Study on structural characterization, physicochemical properties and digestive properties of euryale ferox resistant starch, Food Chem. 359 (2021) 129924.
[11] A. Pasqualone, M. Costantini, R. Labarbuta, C. Summo, Production of extruded-cooked lentil flours at industrial level: effect of processing conditions on starch gelatinization, dough rheological properties and techno-functional parameters, LWT Food Sci. Technol. 147 (2021) 111580.
[12] J. Wu, D.J. McClements, J. Chen, X. Hu, C. Liu, Improvement in nutritional attributes of rice using superheated steam processing, J. Funct. Foods 24 (2016) 338–350.
[13] S.Y. Sim, A.A.N. Aziah, L.H. Cheng, Characteristics of wheat dough and Chinese steamed bread added with sodium alginates or konjac glucomannan, Food Hydrocoll. 25 (2011) 951–957, https://doi.org/10.1016/j.foodhyd.2010.09.009.
[14] D.M.R. Georget, P.S.J. Belton, Effects of temperature and water content on the secondary structure of wheat gluten studied by FTIR spectroscopy, Biomacromolecules 7 (2006) 469–475, https://doi.org/10.1021/bm050667j.
[15] X. Gao, T. Liu, J. Yu, L. Li, Y.i. Feng, X. Li, Influence of high-molecular-weight glutenin subunit composition at Glu-B1 locus on secondary and micro structures of gluten in wheat (Triticum aestivum L.), Food Chem. 197 (2016) 1184–1190.
[16] C.-W. Han, M. Ma, H.-H. Zhang, M. Li, Q.-J. Sun, Progressive study of the effect of superfine green tea, soluble tea, and tea polyphenols on the physico-chemical and structural properties of wheat gluten in noodle system, Food Chem. 308 (2020) 125676.
[17] Zhu, Impact of ultrasound on structure, physicochemical properties, modifications, and applications of starch, Trends Food Sci. Technol. 43 (2015) 1–17, https://doi.org/10.1016/j.tifs.2014.12.008.
[18] R. Thakur, P. Pristijono, C.J. Scarlett, M. Bowyer, S.P. Singh, Q.V. Vuong, Starch-based films: Major factors affecting their properties, Int. J. Biol. Macromol. 132 (2019) 1079–1089.
[19] K. Jochym, J. Kapusniak, R. Barczynska, K. Śliżewska, New starch preparations resistant to enzymatic digestion, J. Sci. Food Agric. 92 (4) (2012) 886–891.
[20] Q. Liang, X. Chen, X. Ren, X. Yang, H. Raza, H. Ma, Effects of ultrasound-assisted enzymolysis on the physicochemical properties and structure of arrowhead-derived resistant starch, LWT 147 (2021) 111616.
[21] X.J. Lian, L.Z. Liu, J.J. Guo, et al., Screening of seeds prepared from retrograded potato starch to increase retrogradation rate of maize starch, Int. J. Biol. Macromol. 60 (2013) 181–185, https://doi.org/10.1016/j.ijbiomac.2013.05.025.
[22] C. Zhong, Y. Xiong, H. Lu, S. Luo, J. Wu, J. Ye, C. Liu, Preparation and characterization of rice starch citrates by superheated steam: A new strategy of producing resistant starch, LWT Food Sci. Technol. 154 (2022) 112890.
[23] W. Li, Z. Zhou, S. Fan, et al., Formation of type 3 resistant starch from mechanical activation-damaged high-amylose maize starch by a high-solid method, Food Chem. 363 (2021), https://doi.org/10.1016/j.foodchem.2021.130344.
[24] D. Li, N.a. Yang, Y. Jin, Y. Zhou, Z. Xie, Z. Jin, X. Xu, Changes in crystal structure and physicochemical properties of potato starch treated by induced electric field, Carbohydr. Polym. 153 (2016) 535–541.
[25] S.R. Falsafi, Y. Maghsoudlou, M. Aalami, S.M. Jafari, M. Raeisi, Physicochemical and morphological properties of resistant starch type 4 prepared under ultrasound and conventional conditions and their in-vitro and in-vivo digestibilities, Ultrasonics - Sonochemistry 53 (2019) 110–119.
[26] M. Gou, H. Wu, A.S.M. Saleh, L. Jing, Y. Liu, K. Zhao, C. Su, B.o. Zhang, H. Jiang, W. Li, Effects of repeated and continuous dry heat treatments on properties of sweet potato starch, Int. J. Biol. Macromol. 129 (2019) 869–877.
[27] W. Liu, Y. Zhang, R. Wang, J. Li, W. Pan, X. Zhang, W. Xiao, H. Wen, J. Xie, Chestnut starch modification with dry heat treatment and addition of xanthan gum: Gelatinization, structural and functional properties, Food 124 (2022) 107205.
[28] Z. Guo, S. Zeng, X.u. Lu, M. Zhou, M. Zheng, B. Zheng, Structural and physicochemical properties of lotus seed starch treated with ultra-high pressure, Food Chem. 186 (2015) 223–230.
[29] X. Wang, F. Lu, C. Zhang, Y. Lu, X. Bie, Y. Xie, Z. Lu, Effects of recombinated anabaena sp. Lipoxygenase on the protein component and dough property of wheat flour, J. Agric. Food Chem. 62 (40) (2014) 9885–9892.
[30] C.-C. Wang, Z. Yang, X.-N. Guo, K.-X. Zhu, Effects of insoluble dietary fiber and ferulic acid on the quality of steamed bread and gluten aggregation properties, Food Chem. 364 (2021) 130444.
[31] Q. Wang, Y. Li, F. Sun, X. Li, P. Wang, J. Sun, J. Zeng, C. Wang, W. Hu, J. Chang, M. Chen, Y. Wang, K. Li, G. Yang, G. He, Tannins improve dough mixing properties through affecting physicochemical and structural properties of wheat gluten proteins, Food Res. Int. 69 (2015) 64–71.
[32] S. Tian, Y. Sun, Influencing factor of resistant starch formation and application in cereal products: A review, Int. J. Biol. Macromol. 149 (2020) 424–431.
[33] P.-H. Hsieh, Y.-M. Weng, Z.-R. Yu, B.-J. Wang, Substitution of wheat flour with wholegrain flours affects physical properties, sensory acceptance, and starch digestion of Chinese steam bread (Mantou), LWT Food Sci. Technol. 86 (2017) 571–576.
[34] E. Yaver, N. Bilgiçli, Effect of ultrasonicated lupin flour and resistant starch (type 4) on the physical and chemical properties of pasta, Food Chem. 357 (2021) 129758.
[35] S. Hedayati, M.J.F.H. Niakousari, Microstructure, pasting and textural properties of wheat starch-corn starch citrate composites, Food Hydrocoll. 81 (2018) 1–5, https://doi.org/10.1016/j.foodhyd.2018.02.024.
[36] E. Lancelot, J. Fontaine, J. Grua-Priol, A. Assaf, G. Thouand, A. Le-Bail, Study of structural changes of gluten proteins during bread dough mixing by Raman spectroscopy, Food Chem. 358 (2021) 129916.
[37] J.E. Bock, S. Damodaran, Bran-induced changes in water structure and gluten conformation in model gluten dough studied by Fourier transform infrared spectroscopy, Food Hydrocoll. 31 (2013) 146–155, https://doi.org/10.1016/j.foodhyd.2012.10.014.